9

Magnetic Fields on Asteroids and Planetesimals

AARON SCHEINBERG, ROGER R. FU, LINDA T. ELKINS-TANTON, BENJAMIN P. WEISS, AND SABINE STANLEY

9.1 Introduction

Extraterrestrial planetary magnetism was first confirmed when Burke and Franklin (1955) detected non-thermal radio emissions attributable to charged particles accelerating in Jupiter's rotating magnetosphere. During the second half of the twentieth century, exploratory missions revealed that planetary magnetic fields were quite common and that the characteristics of each planet's magnetic field were remarkably diverse (Ness, 2010).

Active dynamos are observationally confirmed within Mercury, Earth, Ganymede, and all four giant planets. Remote sensing and paleomagnetic studies indicate the past existence of internally generated magnetic fields on Mars and the Moon despite the lack of present-day dynamos (Acuña *et al.*, 2008; Weiss and Tikoo, 2014). Magnetization of meteorites indicates that planetesimals also likely generated transient dynamos (Weiss *et al.*, 2010), and the nebula itself contained a large-scale magnetic field (Fu *et al.*, 2014b).

A better understanding of the evolution of dynamo fields in planetesimals provides a context with which to interpret future paleomagnetic, geochemical, and geophysical observations. Increased understanding of these ancient terrestrial dynamos can in turn aid our understanding of dynamos presently active in our solar system and inform modeling of potential exoplanetary dynamos.

In this chapter, we summarize the present state of observation and theory of magnetism in these small bodies. First, we summarize the methods and results of paleomagnetism studies of meteorite samples and *in situ* observation of asteroids. Next, we examine the conditions necessary for core formation, a prerequisite of dynamo action. We then summarize dynamo theory and its implementation in numerical modeling, focusing particularly on planetesimal dynamos. Following this, we consider the effect of core crystallization on core dynamos. We conclude with a discussion of alternative proposed explanations for meteorite magnetization.

9.2 Meteoritic Paleomagnetism

Meteorites with a wide diversity of compositions and geologic histories have been recovered on Earth. These samples include both unmelted accretionary rocks known as chondrites and partially and fully melted igneous rocks known as achondrites (Weisberg *et al.*, 2006). As such, meteorites contain records of the formation and evolution of solid bodies in the early solar system.

Paleomagnetism is an experimental technique for reconstructing the nature of ancient magnetic fields based on the measurement of remanent magnetization in geologic samples. Paleomagnetic studies of meteorites can thereby investigate magnetic fields on small bodies in the early solar system.

Because ferromagnetic minerals are present in nearly all natural rocks, a range of processes can impart a magnetic remanence that may persist for the age of the solar system. Due to the high-temperature processes experienced by meteorites and their inclusions both in the solar nebula and parent bodies, most magnetization in such samples has been interpreted as thermoremanent magnetization (TRM; e.g. Weiss *et al.*, 2010). In the TRM acquisition process, electron spins in ferromagnetic mineral grains in a sample become preferentially aligned to the background magnetic field during cooling through temperatures below the Curie point, thereby producing magnetization. The magnetization intensity is directly proportional to the intensity of the background magnetic field for field strengths corresponding to most natural environments. Therefore, paleomagnetic characterization of TRM can potentially constrain the intensity of ancient magnetic fields on asteroidal bodies.

Despite this theoretical potential and the availability of high-precision instrumentation (e.g. Fu *et al.*, 2014a; Bryson *et al.*, 2015), the recovery of reliable paleomagnetic data remains challenging for meteoritic materials. The principal source of uncertainty surrounding studies of meteoritic magnetism is the ubiquity of remagnetization processes on their parent bodies and after their arrival on the Earth. Strong shock above several to ten GPa may lead directly to remagnetization or induce sufficient heating to destroy pre-existing magnetization (Gattacceca *et al.*, 2008). At the same time, although entry through the Earth's atmosphere leads only to remagnetization of material within several millimeters of the fusion crust surface (Sears, 1975), exposure to strong artificial magnets and terrestrial weathering after the meteorite's arrival routinely render the pre-existing remanence unrecoverable.

As such, the identification and interpretation of extraterrestrial remanent magnetization in meteoritic samples hinge on the application of both paleomagnetic and non-paleomagnetic proxies to understand the thermal, alteration, and shock history of samples. Mineralogical indicators can reveal the occurrence of shock greater than ~5 GPa, which may affect the sample's magnetic record (Gattacceca

et al., 2008; Stöffler *et al.*, 1991). Meanwhile, paleomagnetic measurements of the magnetization intensity can be used to identify and exclude magnetization introduced by exposure to strong artificial magnetic fields (Weiss *et al.*, 2010). Finally, the fusion-crust baked contact test, which looks for systematic variation of the remanent magnetization from samples located progressively farther from the fusion-crust surface, represents a robust method of confirming the extraterrestrial origin of magnetization in meteorite interiors (Nagata, 1979).

For meteorites in which the experiments described above indicate the presence of extraterrestrial magnetization, dating techniques such as ^{40}Ar–^{39}Ar thermochronology permit the description of the meteorite's thermal history and constrain the timing of TRM acquisition by the sample (e.g. Shea *et al.*, 2012; Fu *et al*., 2012). Equally important are mineralogical indicators that permit estimation of the timescale of cooling and, therefore, of remanence acquisition (e.g. Grove, 1982). This information constrains the temporal stability of the magnetic field environment on the parent body, which is potentially a key distinguishing characteristic between long-lived internal dynamo fields and transient fields from plasmas generated by impacts or present in the external nebula.

9.2.1 Magnetic Fields Recorded in Meteorites

The techniques described above permit the identification of secondary overprints that may otherwise be confounded with any primary remanent magnetization recording asteroidal magnetic fields. Even so, early studies of meteorites revealed that the ferromagnetic mineralogy of some meteorite classes is poorly suited for recording ambient magnetic fields. Subsolidus recrystallization of Ni-rich metal in ordinary chondrites, even under low metamorphic heating, results in the erasure of pre-existing remanence and possibly the formation of tetrataenite, which may not record an early magnetic field if it formed late in the history of the body (Morden and Collinson, 1992; Gattacceca *et al.*, 2003; Uehara *et al.*, 2011).

Later studies of howardite–eucrite–diogenite (HED) meteorites showed that some samples carry a unidirectional magnetization consistent with the presence of a stable magnetic field with intensity order 10 μT on the HED parent body, likely the asteroid (4) Vesta *(*Collinson and Morden, 1994; Cisowski, 1991; Morden, 1992). However, due to the lack of direct age dating, detailed petrographic constraints on shock and cooling history, and possible contamination by fusion crust material, an unambiguous identification of the source of the magnetizing field, remained elusive.

Subsequent paleomagnetic studies of HEDs and other achondrite groups have introduced more robust room-temperature paleointensity protocols (Gattacceca and Rochette, 2004) and employed a range of petrography and thermochronology

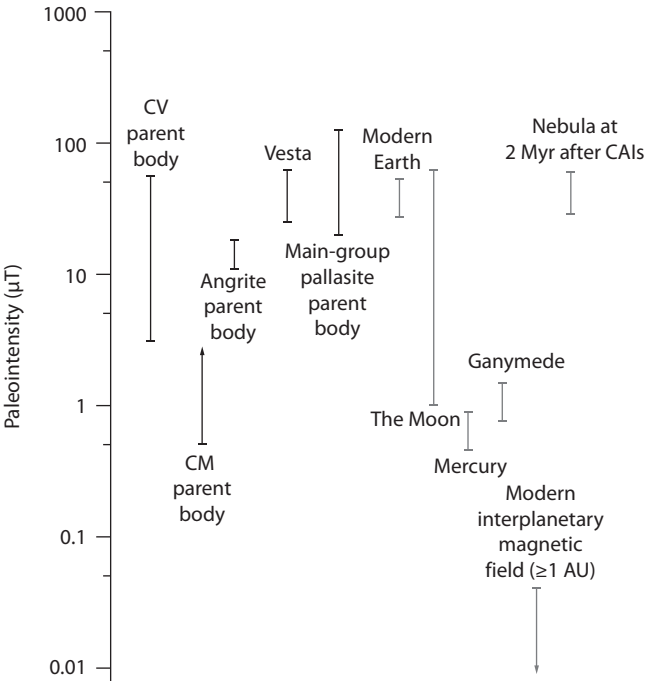

Figure 9.1 Summary of surface dynamo magnetic field strengths on small bodies and terrestrial planets. Nebular and modern interplanetary magnetic fields are included for reference. Data from Kivelson *et al.* (1996), Carporzen *et al.* (2011), Anderson *et al.* (2011), Emmerton *et al.* (2011), Tarduno and Cottrell (2012), Fischer *et al.* (2013), Tarduno *et al.* (2012), Fu *et al.* (2014b), Weiss and Tikoo (2014), Bryson *et al.* (2015), and Cournede *et al.* (2015).

techniques to identify the origin of any recorded magnetic fields. Such experiments have shown that angrites, a small group of basaltic achondrites, have avoided the strong shock, recrystallization, and terrestrial processes affecting other meteorites and that they cooled in the presence of a stable ~10 μT magnetic field most likely generated by a magnetic core dynamo (Weiss *et al.*, 2008) (Figure 9.1). A more recent study of the eucrite ALHA81001 has shown that the stable magnetic fields with intensity greater than ~2 μT existed on the surface of Vesta at 3.7 Ga, suggesting the presence of an earlier dynamo magnetic field that magnetized portions of the Vestan crust (*Fu et al.*, 2012). Finally, *Tarduno et al.* (2012) and *Bryson et al.* (2015) showed that strong magnetic fields of up to ~100 μT existed on the main-group pallasite parent body, indicating the persistence of a core dynamo for several hundred Myr. Together, these studies suggest that early-accreting, fully differentiated planetesimal-sized bodies were capable of harboring magnetic-core dynamos.

Records of strong parent-body magnetic fields have also been observed in carbonaceous chondrites. A dynamo origin for the magnetization of chondritic material would imply that its parent body partially differentiated, forming a metallic core, while the crust remained primitive (Elkins-Tanton *et al.*, 2011).

Early studies of the Allende CV carbonaceous chondrite revealed a unidirectional remanent magnetization acquired in a magnetic field of several tens to 100 μT (Butler, 1972; Sugiura *et al.*, 1979; Wasilewski, 1981). More recent paleomagnetic experiments have replicated this result (Emmerton *et al.*, 2011; Carporzen *et al.*, 2011). Furthermore, Carporzen *et al.* (2011) used a combination of I–Xe thermochronology and high-resolution thermal demagnetization to argue that the most likely explanation for the remanent magnetization in Allende is a magnetization overprint due to metamorphic heating and/or aqueous alteration in a core dynamo magnetic field with intensity >20 μT. Subsequent modeling work has argued that a metamorphic TRM may be the result of impact heating during the presence of impact-generated magnetic fields (Bland *et al.*, 2014). However, the uniformity of the blocking temperature of the observed remanent magnetization in Allende (<10 °C differences at between 1-mm and 1-dm scales) is unlikely to be consistent with the heterogeneous temperature fields predicted by the Bland *et al.*, (2014) impact heating model (Carporzen *et al.*, 2011; Fu *et al.*, 2014a). Finally, measurements of isolated Allende chondrules, some of which experienced prolonged aqueous alteration (Swindle, 1998), suggests that any core dynamo in the CV parent body had decayed by the time of the latest alteration event (Fu *et al.*, 2014a), which may have occurred up to ~40 Myr after the formation of calcium–aluminum inclusion (CAIs; Carporzen *et al.*, 2011).

Experiments on other carbonaceous chondrite groups have revealed further evidence for stable magnetic fields on their parent bodies. A study of seven CM chondrites revealed unidirectional magnetic remanence acquired in a ~2-μT magnetic field (Cournède *et al.*, 2012), although the early formation ages of CM chondrites within 4 Myr of CAIs prevents an unambiguous distinction between a parent-body dynamo and a solar nebula origin for the magnetic field (see Section 9.6.2). Meanwhile, a preliminary study of R chondrites yielded similar paleointensities of ~5 μT, which, when combined with I–Xe geochronology, suggests the persistence of a core dynamo >10 Myr after CAIs (Cournede *et al.*, 2014).

A number of both chondritic and achondritic parent bodies show no evidence for past dynamo activity. Metamorphic heating of the Semarkona LL chondrite to ~200 °C should have imparted a unidirectional magnetization in the mineralogically pristine dusty olivine inclusions if the metamorphism coincided with an active dynamo. No such magnetization was observed in isolated dusty olivines (Fu *et al.*, 2014a). Among experiments on achondrites, the ungrouped meteorite NWA 7325 cooled in a magnetic field with intensity <2 μT and consistent with

0 μT (Weiss *et al.*, 2014). These experiments suggest that dynamo generation may not have occurred universally in differentiated bodies, possibly due to variations in the style and timescale of core cooling (Nimmo, 2009).

9.2.2 Magnetic Fields in Asteroids

Paleomagnetic studies of meteorites and theoretical considerations indicate that some differentiated asteroids were magnetized by an internal core dynamo (Weiss *et al.*, 2010; Nimmo, 2009) while undifferentiated asteroids and comets could have been magnetized while accreting in the presence of a solar nebula magnetic field (Fu and Weiss, 2012). *In situ* magnetic field measurements of asteroids should enable important tests of these processes by extending magnetic measurements to much larger spatial scales than can be achieved from laboratory studies of meteorites. Such large spatial scales could be used to constrain the temporal variability and geometry of the dynamo.

There is in fact much reason to think that asteroid fields should be detectable by spacecraft magnetometers. Greenstadt (1971a; 1971b) and subsequent authors (Baumgartel *et al.*, 1997; Omidi, *et al.*, 2002) have shown that for a main-belt asteroid to stand off the solar wind and generate a magnetosphere, a global magnetic moment of at least ~10^{15} A m^2 is required. Assuming a uniformly magnetized body, this would correspond to specific magnetizations of ~10^2, 0.1, and 10^{-4} A m^2 kg^{-1} for asteroid radii of 1, 10, and 100 km, and assuming a bulk density of 2500 kg m^{-3} (Figure 9.2). Given that the natural remanent magnetizations (NRMs) of known chondrites range between 10^{-5} and 10^{-1} A m^2 kg^{-1} (with samples having $>10^{-2}$ A m^2 kg^{-1} likely remagnetized by hand magnets) while only stony-iron and iron meteorites have NRM $>10^{-1}$ A m^2 kg^{-1}, minimum radii of ~100 km for chondritic bodies and ~10 km for metallic bodies are expected for an asteroid to have a magnetosphere (Figure 9.2).

Furthermore, weaker asteroidal magnetization could still be detected indirectly from observations of solar-wind disturbances during a spacecraft flyby (Greenstadt, 1971a; 1971b). In particular, it has been shown that asteroids with magnetic moments exceeding 10^{12} A m^2 (corresponding to specific magnetizations of 10^{-1}, 10^{-4}, and 10^{-7} A m^2 kg^{-1} for asteroid radii of 1, 10, and 100 km and a density of 2500 kg m^{-3}) can generate solar-wind plasma waves that could be detected downstream from the asteroid (Baumgartel *et al.*, 1997; Omidi *et al.*, 2002; Figure 9.2b).

The above discussion optimistically assumes that the asteroids are uniformly magnetized, which is unlikely given that most asteroids are fragmented and that the direction of magnetizing fields were likely not steady. Nonunidirectionally magnetized asteroids would be required to have fine-scale NRM intensities

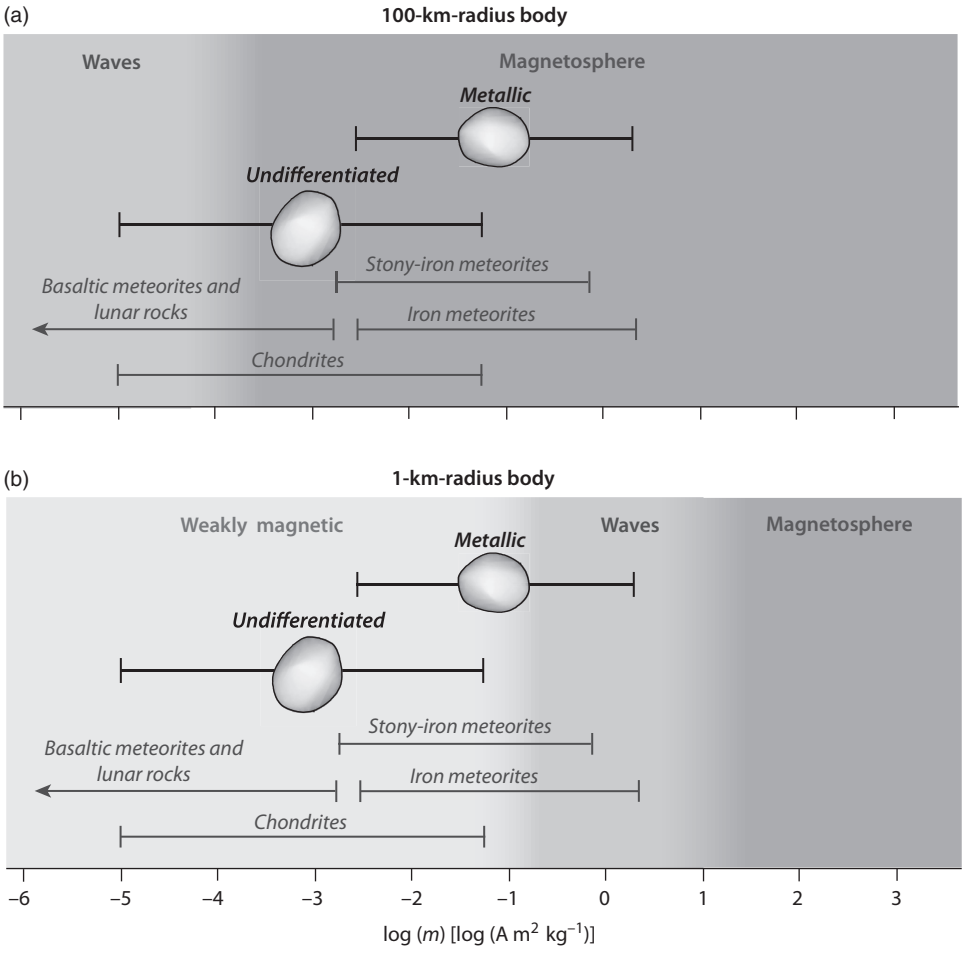

Figure 9.2 Conditions for detecting signatures of asteroid magnetization as a function of asteroid magnetization for (a) a 100-km-radius body and (b) a 1-km-radius body. Three possible detection regimes are: the asteroid forms a magnetospheric cavity (red), the asteroid generates plasma waves (blue), or the asteroid has weak fields only detectable from a very close approach (green). The range of observed NRMs for various meteorite types is shown at the bottom (data from *Pesonen et al.*, 1993). For each asteroid size, two asteroid compositions are shown: metallic and undifferentiated (i.e. chondritic body). The metallic body in (a) is representative of asteroid (16) Psyche. After *Greenstadt* (1971a; 1971b), *Baumgartel et al.* (1997), and *Auster et al.* (2010). A black and white version of this figure will appear in some formats. For the colour version, please refer to the plate section.

considerably higher (potentially by orders of magnitude) than the values listed above. As a result, close approaches by spacecraft like flybys or landings are essential for detecting asteroid magnetic fields, and a lack of detection makes it very difficult to exclude substantial fine-scale nonunidirectional magnetization.

Magnetometer flybys have been conducted near the asteroids (21) Lutetia, (243) Ida, (951) Gaspra, (2867) Šteins, and (9969) Braille (Richter *et al.*, 2012; Kivelson *et al.*, 1995) and spacecraft with magnetometers have landed on the asteroid (433) Eros and the comet 67P/Cheryumov–Gerasimenkov (Auster *et al.*, 2015). Impressively, none have unambiguously detected a remanent field from these bodies, with the latter two missions constraining the surface field to less than a few nT.

A possible exception is Deep Space 1's flyby of the 0.78-km-radius Q/S-type asteroid (9969) Braille, which observed a weak (~1–2 nT) change in the ambient magnetic field upon its closest approach of 28 km (Richter *et al.*, 2001). However, this field change is near the sensitivity limit of the investigation. Another possible exception is Galileo's flyby of the 8-km-radius S-type asteroid 951 Gaspra, during which it was thought to have detected magnetic field rotations produced by interaction of the solar wind with an intrinsic asteroidal magnetic field (Kivelson *et al.*, 1993, 1995). However, it has subsequently been proposed that the observed plasma waves do not require the presence of a significant asteroidal magnetic field but could rather be explained purely by variability of the background solar wind (Blanco-Cano *et al.*, 2003).

The lack of magnetic field detections near some of these asteroids places stringent constraints on the total magnetic moments of these asteroids. In particular, if it is assumed that the asteroids are uniformly magnetized, then the inferred upper limit on the magnetizations of asteroids (21) Lutetia (Richter *et al.*, 2012), (433) Eros (Acuña *et al.*, 2002), and comet 67P/Cheryumov–Gerasimenkov (Auster *et al.*, 2015) are below that measured for virtually all known meteorites. This means that either these bodies are made of materials not yet recognized among meteoritic materials on Earth or, more likely, they are made of materials resembling known meteorites but are nonunidirectionally magnetized at spatial scales exceeding that of meteorite hand samples (>10 cm, Wasilewski *et al.*, 2002). Therefore, magnetic field measurements of asteroids do not presently support or refute the inference made from meteorite paleomagnetic studies that many asteroids likely generated dynamo magnetic fields.

9.3 Core Formation

The presence of an advecting liquid core is necessary to generate an internal dynamo. However, differentiation into a silicate mantle and liquid metal core is not universal on small bodies. Here, we summarize how and under what conditions this prerequisite is satisfied. Metal–silicate differentiation in an initially chondritic parent body produces a primary core. Later accretionary impacts involving partially differentiated bodies would result in mechanical and chemical mixing of the cores. The degree of chemical equilibrium such a hybrid core could have

with its equally hybrid silicate exterior could be complex. We will address only primary cores, which, in contrast, form from the same initial bulk material as their silicate exteriors.

The Fe–FeS eutectic occurs at 31 wt% sulfur (equivalent to 85% FeS and 15% Fe) and at a temperature of 988 °C (Brett and Bell, 1969). Initial melting will therefore occur at that temperature, with subsequent melting and core formation dependent upon the sulfur content of the body (Fei *et al.*, 1997). The planetesimal is presumably heated by the short-lived isotope ^{26}Al. The time to reach that temperature depends upon the initial ^{26}Al content, the size of the body, and the rate of accretion.

Investigations of meteorites using the Hf–W isotopic system show that the Fe–Ni metal cores of planetesimals formed very rapidly in the early solar system, in some cases within hundreds of thousands of years of the first (Scherstén *et al.*, 2006). For a 100-km-radius planetesimal instantaneously accreting at the time of first CAIs, the eutectic melting temperature of FeS is reached in about 100 000 years (Fu and Elkins-Tanton, 2014), consistent with the measured early formation ages.

Direct observations of primitive achondrites, which display incomplete segregation of a Fe,Ni–S melt, show that efficient transport of differentiating melts occurs at or below 5% whole rock melt fraction or at ~1250 °C (McCoy *et al.*, 1997). For lower melt fractions, debate continues over whether the FeS liquid alone can percolate downward to form a core, perhaps aided by deformation (Yoshino *et al.*, 2003), without substantial melting of the silicates. Deformation appears to aid segregation of an FeS liquid, though small degrees of silicate melt hinders FeS segregation (Cerantola *et al.*, 2015). Cerantola *et al.* (2015) find that about 90% of the liquid FeS can drain from the mantle through deformation, but complete core formation requires a magma ocean stage.

At about the same temperatures as the initial melting and segregation of the metal component, hydrated silicate minerals will be heated beyond their stability ranges and will expel a fluid phase. This fluid phase may interact with the metal component in previously uninvestigated ways. The fluid may contain significant carbon and sulfur.

Iron meteorites are relatively sulfur-poor, while chondritic meteorites are in general far richer in sulfur. Tomkins *et al.* (2013) found that fractionation drove the Campo del Cielo IAB group of non-magmatic irons to a system with immiscible iron carbide and iron sulfide liquids, which allowed the silicate fraction to retain the sulfur as it separated from the iron fraction. The Campo del Cielo IAB group has been proposed to have solidified from melts produced in impact processes, rather than in a fractionally solidifying core, but the process of sulfur segregation may well be implicated in core formation as well as in impact-produced non-magmatic iron meteorites. Several fluid phases may be

implicated, including the hydrous fluid expelled from silicate minerals, and the immiscible carbide and sulfide liquids.

Planetesimals likely experienced an initial core-forming process when the inside of the growing body reached a temperature that allowed metal segregation, but under the low gravity, and in the absence of a magma ocean, segregation would have been sluggish. This initial process likely included interactions with fluids, and segregation remained incomplete until and unless a magma ocean stage was achieved in the overlying silicates. In agreement with this model, tungsten systematics in magmatic iron meteorites indicate that core formation may have occurred over an interval of about a million years, beginning with segregation of Fe–FeS from silicates and continuing with segregation of Fe–Ni liquid (*Kruijer et al.*, 2014).

The assumption of a single core-forming event is probably an oversimplification even for primary cores in planetesimals. The ongoing impacts would have increased the size of the body, and these added materials might or might not have reached temperatures sufficient to drain their metals into the planetesimal core. In some cases, impacts could have disrupted accretion (and core formation) through hit-and-run collisions, as in *Asphaug* (2010).

9.4 Planetesimal Dynamos

A dynamo is a process that converts mechanical work produced by flow of an electrically conducting fluid into magnetic energy. The theory has been widely successful and is the commonly accepted explanation for the observed internally produced magnetic fields of stars and planets. The conducting fluid varies: plasma (stars), metallic hydrogen (Jupiter and Saturn), and water/ammonia/methane (Uranus and Neptune). In terrestrial planets and planetesimals, convection in a molten iron core is the most readily available explanation. A silicate magma ocean dynamo has also been proposed for Mars (Stevenson, 2001) and for early Earth (Ziegler and Stegman, 2013), but this mechanism is implausible in small bodies since it invokes high pressures to sufficiently enhance the silicate material's electrical conductivity.

The field of magnetohydrodynamics (MHD) studies the behavior of such a system by considering Maxwell's equations, which describe the behavior of magnetic and electric fields, in tandem with equations describing conservation of momentum (the Navier–Stokes equations), mass, and energy in fluid flow. The time rate of change of the magnetic field $\vec{B}$ is described by the magnetic induction equation,

$$\left[\frac{\partial}{\partial t}+\vec{u}\cdot\nabla\right]\vec{B}=\lambda\nabla^2\vec{B}+\left(\vec{B}\cdot\nabla\right)\vec{u}-\vec{B}\left(\nabla\cdot\vec{u}\right) \tag{9.1}$$

where $\vec{u}$ is the velocity field and λ is the magnetic diffusivity. This equation can be derived by combining Maxwell's equations with Ohm's law in a moving reference frame and assuming displacement current is negligible. This assumption is accurate as long as fluid speeds are small compared to the speed of light. The left side of the equation is the material derivative of the field. The first term on the right side of the equation can be recognized as a diffusion term. The second and third terms are source terms accounting for the stretching of magnetic field lines due to fluid motion and the fluid's compressibility, respectively.

Using the magnetic induction equation, it can be shown that only certain fluid flow patterns (i.e. certain velocity field solutions) will support a magnetic field, while several of them cannot support a dynamo. Cowling (1934) presented, as the first of several "anti-dynamo" theorems, a proof that an axisymmetric magnetic field (such as an axial dipole) cannot be produced by an axisymmetric flow field. Therefore, dynamos and the convection that drives them must be modeled in three dimensions rather than reducing the number of spatial dimensions, and resulting solutions to the equation are necessarily complex. A fluid flow geometry shown to be very conducive to dynamo action is helical motion, which naturally occurs in core convection due to the rapid rotation and spherical geometry of the core.

Not every flow field capable of producing a dynamo is also physical. The flow field is contained by equations describing conservation of momentum (the Navier–Stokes equations) and conservation of mass:

$$\rho\left[\frac{\partial}{\partial t}+\vec{u}\cdot\nabla\right]\vec{u}=-\nabla p+\frac{1}{\mu_0}\left(\nabla\times\vec{B}\right)\times\vec{B}+\mu\nabla^2\vec{u}+\frac{1}{3}\mu\nabla\left(\nabla\cdot\vec{u}\right)+\rho\vec{g}-2\rho\vec{\Omega}\times\vec{u} \tag{9.2a}$$

$$\frac{\partial\rho}{\partial t}+\nabla\cdot\left(\rho\vec{u}\right)=0 \tag{9.2b}$$

where ρ is fluid density, p is pressure, μ_0 is the permeability of free space, $\vec{\mu}$ is the dynamic viscosity, $\vec{g}$ is gravitational acceleration, and $\vec{\Omega}$ is the body's angular velocity. The left side of the equation is the advective time derivative of the velocity. The terms on the right-hand side represent, from left to right, pressure gradients, Lorentz forces, viscous forces, buoyancy forces, and Coriolis forces. Under the Boussinesq approximation, ρ is assumed constant except in the buoyancy term. In a thermally driven dynamo, buoyancy is due to thermal expansivity. The temperature field of the fluid is governed by:

$$\frac{\partial T}{\partial t}+\vec{u}\cdot\nabla T=\kappa\nabla^2T+\varepsilon \tag{9.3}$$

where T is temperature, κ is thermal diffusivity, and ε is any volumetric temperature source or sink. Together, these four equations govern a convection-driven dynamo.

9.4.1 Modeling Methods

Most numerical models of dynamos solve the above equations in a spectral framework; however, increasing availability of computational resources has allowed for finite-element dynamo modeling to also become feasible (Chan *et al.*, 2007; Zhan *et al.*, 2011). Both methods have their respective challenges and researchers are constantly improving models with state-of-the-art numerical methods.

Numerical models are not capable of fully resolving core fluid motion for the dimensionless parameter values typically found in cores. Dynamo models are thus operated in an unrealistic parameter space. Most importantly, the Ekman number (the nondimensional number characterizing the ratio of viscous forces to the Coriolis forces) and magnetic Prandtl number (which characterizes the ratio of the viscous diffusivity to the magnetic diffusivity) attainable by numerical models are at least eight and four orders of magnitude larger, respectively, than their estimated physical values (Christensen and Wicht, 2007). In effect, a much larger viscosity is assumed in numerical models, which ignores the possible impact of small-scale velocity field features.

Often, studies are concerned only with estimating the order of magnitude of a dynamo's magnetic field. This aim can be achieved by scaling estimates that forego the need for complex fluid dynamical modeling. This method typically relates total magnetic energy density to the energy density thermodynamically available to power a dynamo:

$$\frac{B^2}{2\mu_0} \propto f_{ohm} \frac{L}{U} \varphi \tag{9.4}$$

Here, B is the magnetic field magnitude within the core and f_{ohm} is the fraction of energy converted to magnetic energy and lost by ohmic dissipation. U is its characteristic velocity and L its characteristic lengthscale so that L/U represents the convective timescale. The parameter φ is the volumetric thermodynamically available power, which can be determined from the thermal and composition buoyancy that may be driving convection. U is a more difficult parameter to constrain, since the characteristic velocity depends on which terms in the momentum equation are dominant. Various formulations are used in the literature. The constant of proportionality relating the two sides of the equation is estimated based on observation of known planetary fields and on dynamo modeling (*Christensen*, 2010).

9.4.2 Planetesimal Dynamo Models

Studies of planetesimal dynamos in particular have been limited (Weiss *et al.*, 2008; Nimmo, 2009; Weiss *et al.*, 2010; Elkins-Tanton *et al.*, 2011; Sterenborg and Crowley, 2013; Bryson *et al.*, 2015). They typically employ a scaling law to evaluate field magnitude. To calculate longevity, they assume a critical magnetic Reynolds number, a critical core heat flux, or both. The magnetic Reynolds number is defined as $Re_m = UL/\lambda$. A critical threshold Re_m must be reached for there to be sufficient convective vigor to maintain a dynamo. Studies have placed this value variously from 10 to 100 (Christensen *et al.*, 1999; Stevenson, 2003, Monteux *et al.*, 2011). For purely thermal convection, total core heat flux must exceed adiabatic heat flux.

Nimmo (2009) examined the energetics of asteroidal cores and evaluated the minimum cooling rate required to produce a dynamo. He found that for purely thermal convection, production of a stable magnetic field would require a cooling rate of 1–100 K Myr^{-1}. He also examined the effect of core solidification, which is discussed in the next section; and found that a core greater than 50–150 km in radius would have a sufficiently high Re_m to support a dynamo. This calculation used a conservative threshold value for dynamo action, requiring that $Re_m > 100–1000$.

Elkins-Tanton *et al.* (2011) investigated the conditions under which core heat flux in small bodies sufficed to produce a dynamo. They examined bodies from 50–500 km in radius, assuming a core radius at most half of the total radius, and determined core heat flux as a function of time, accounting for energy from accretion and ^{26}Al radiogenic heating in the mantle. They found that cores over ~50–100 km in radius would have had sufficient core heat flux to power a dynamo for more than 10 Myr.

However, sufficient heat flux is not the only requirement for dynamo action to occur. Sterenborg and Crowley (2013) modeled the thermal evolution of a planetesimal with a convecting mantle and evaluated the potential for dynamo action assuming thermally driven convection (i.e. no core solidification). The magnetic Reynolds number was found to be the limiting factor. They used a critical Re_m of 10–100 and found that core convection in bodies smaller than ~500 km in radius could only produce a dynamo for less than 10 Myr.

9.5 Core Crystallization

Due to the nature of the core accretion process, particularly in the low-gravity environment of planetesimals, newly formed metallic cores were probably entirely molten. As planetesimals cooled, their cores eventually solidified. This solidification process would have strongly affected any dynamo still actively produced in the

core. However, crystallization in a low-gravity core is potentially very complex, and many scenarios remain unexplored. As such, the nature of a dynamo during this phase of planetesimal history, and the potential for remanent magnetism to preserve a record of this field, are unknown. In this section, we first summarize the physics of core crystallization and then discuss its impact on dynamos.

9.5.1 Physics of Core Crystallization

The core liquidus and solidus temperatures depend on both composition and pressure. Just as for core formation, sulfur's particularly large effect on melting temperature has major implications for the solidification process. In a purely Fe–FeS system, which for simplicity is often assumed in planetary cores, the liquidus decreases from 1538 °C for pure Fe to 988 °C at its eutectic composition at ambient pressure (Kullerud and Yoder, 1959). On the other hand, pressure effects are not likely to alter the liquidus by more than a few degrees across a planetesimal core.

The liquidus and the adiabatic temperature profile of a convecting core both depend on depth. In high-pressure systems (i.e. larger bodies), the center of the core reaches the liquidus first and crystallization forms a solid inner core and proceeds outward. Williams (2009) suggested that, in bodies with core pressures less than around 4 GPa, the outer boundary of the core would reach the liquidus first and thus solidification would proceed inward. Solidification would also proceed from the outer edge of the core if cooling was sufficiently rapid. However, since the liquidus is highly composition-dependent and almost negligibly dependent on depth, the mode of solidification may be more complex, occurring, for example, at all depths or with substantial lateral heterogeneity.

The cooling rates and Ni fraction of iron meteorites can provide some insight into the direction of crystallization. For a given parent body, cooling rates will be lowest for those meteorites that originated near the body's center. Because nickel is preferentially partitioned into the remaining liquid as iron solidifies, the earliest solids will have a lower Ni fraction than later solids. Therefore, the positive correlation between Ni fraction and cooling rate in the IVB meteorite family indicates that the parent body solidified from the center outward (Yang *et al.*, 2010), while the inverse correlation in the IVA family indicates inward solidification (Yang *et al.*, 2008).

To complicate the process further, sulfur is incompatible with the crystallizing iron. As metal solidifies, the remaining melt is enriched in sulfur until the eutectic point, when FeS (troilite) also forms. Melt enriched in sulfur is buoyant and could concentrate at the liquid core's outer boundary, decreasing the local solidus and thus inhibiting inward solidifcation. This effect could lead to large-scale

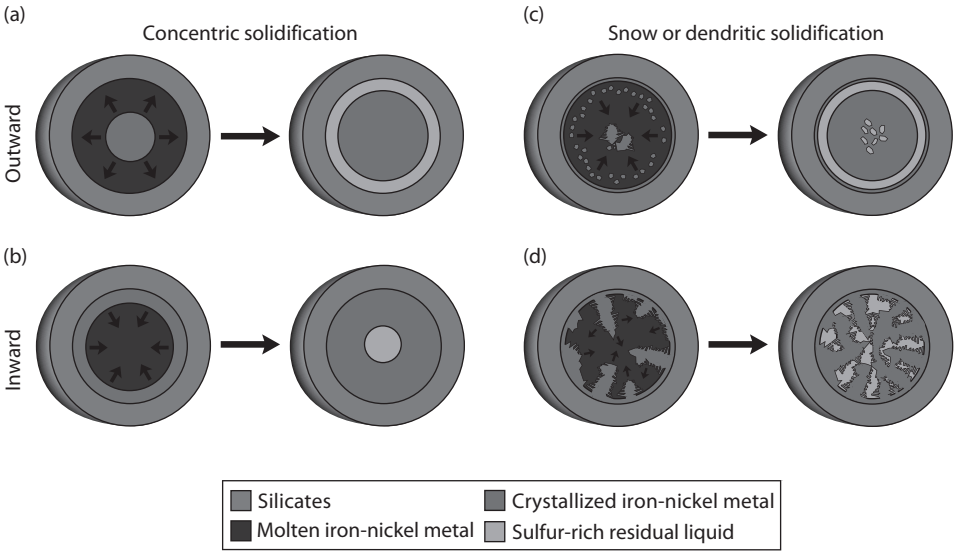

Figure 9.3 Four potential core solidification scenarios and their resulting end-states. (a) Outward (Earth-like) solidification. (b) Concentric inward solidification. (c) Outward solid core growth due to accumulated iron "snow" and/or destabilized dendrites. (d) Dendritic inward solidification. Figure from Scheinberg *et al.* (2015). A black and white version of this figure will appear in some formats. For the colour version, please refer to the plate section.

dendritic growth (Haack and Scott, 1992; Narayan and Goldstein, 1982), though such dendrites may be unstable even in the low-gravity field of a planetesimal core.

Chabot and Haack (2006) and Goldstein *et al.* (2009) review the supporting evidence for both outward and inward core solidification, which could occur dendritically or concentrically. Crystals may also form as free-floating "snow" within the liquid and settle to form a cumulate inner core (Scheinberg *et al.*, 2016). Such iron snow may also remelt, as has been explored for Mercury, the Moon, and Ganymede (e.g. Hauck *et al.*, 2006; Laneuville *et al.*, 2014; Christensen, 2014). These four scenarios are illustrated in Figure 9.3.

9.5.2 Dynamos During Core Crystallization

Outward concentric core solidification typical of larger cores provides two additional power sources for dynamo action. First, latent heat of fusion is released at the inner core boundary. Second, light elements such as sulfur are expelled from the boundary, reducing the density of the nearby liquid. Both these buoyancy terms enhance convection and therefore the dynamo. Christensen *et al.* (2009) estimated that over half of the power available to the Earth's dynamo is a result of solidification.

Nimmo (2009) found that, in planetesimals, this additional buoyancy reduced the core cooling rate necessary to sustain a dynamo by three orders of magnitude. Bryson *et al.* (2015) found that such a thermochemical dynamo could be long-lived, lasting up to 25–150 Myr depending on the object's size.

Scheinberg *et al.* (2016) studied the effect of core crystallization on mantle-less planetesimal dynamos for alternative solidification scenarios. Rather than enhancing convection, inward solidification was found to reduce it by inserting both latent heat and light elements at the upper boundary of the convective region. This effect rendered fractional concentric inward solidification infeasible, although a weakened dynamo was still possible in cores larger than 100 km in radius assuming sufficient trapped melt between inwardly growing dendrites.

Conversely, free-floating crystal formation and settling (the cumulate inner core scenario) would enhance the dynamo. Although latent heat and chemically buoyant liquid would still inhibit convection, the negative buoyancy of the free-floating metal crystals is sufficient to cause a net increase in power available for convection and for dynamo action.

However, these crystals are likely to remelt (the iron-snow scenario). In that case, the zone in which crystallization occurs would gradually thicken and would be stably stratified. When these crystals melt, they would increase the density of the surrounding liquid, thereby causing convection in the region beneath it and potentially driving a dynamo (Rückriemen *et al.*, 2015).

These various scenarios are not mutually exclusive; outward solidification, inward solidification, and iron snow could all have occurred in the same body, perhaps simultaneously, with unknown consequences for the dynamo.

Finally, inward solidification raises the possibility that a solid outer metal shell could have cooled below its Curie temperature and thus recorded the magnetic field produced in an underlying liquid core. Such a magnetized shell could in turn affect the dynamo and the magnetization of nearby material. These questions remain unexplored.

9.6 Alternative Magnetization Mechanisms

Although thermochemical convection is most often the assumed source of magnetization, other mechanisms have also been proposed. Here, we discuss alternative dynamo power sources as well as the larger solar nebula context.

9.6.1 Dynamo Alternatives to Core Convection

Convection is a likely source of the fluid motions producing dynamo action, but it can be limited in timescale because it only occurs while the core is cooling.

Especially for small bodies like planetesimals, this timescale can be as short as millions of years (Weiss *et al.*, 2008). However, dynamo action may occur without core cooling if mechanical forcing is present. For example, precession and libration have been shown to produce flow instabilities capable of dynamo action (e.g. Kerswell, 1993; Tilgner, 2005), as have impact-generated torques (Le Bars *et al.*, 2011; Wei *et al.*, 2014).

These mechanisms may be more relatively important for small-body dynamos than for planets for two reasons. First, impact frequency was significantly higher in the early solar system. Second, since the core–mantle boundary of planetesimals is likely to be less spherical due to lower gravity, additional instabilities may be produced from the topography at this boundary in these bodies.

Petrographic and geochronological constraints on the timescale over which the magnetization is acquired (e.g. Shea *et al.*, 2012) may potentially distinguish between a long-lived thermochemical convection dynamo and shorter-lived impact-related processes.

9.6.2 The Solar Nebula Magnetic Environment

A rotating body embedded in a net magnetic field during the timespan of cooling may acquire a TRM parallel to the axis of rotation (Suavet *et al.*, 2009). Therefore, the paleomagnetic record recovered from early-forming planetesimals that acquired remanent magnetization during the presence of the solar nebula may reflect both magnetic core dynamo-generated and externally produced magnetic fields.

Analysis of isolated dusty olivine-rich chondrules from the Semarkona LL chondrite suggests that nebular magnetic field intensities are between 5 and 50 μT in the formation region of the measured chondrules (Fu *et al.*, 2014b). However, these measurements provide no constraint on the stability of the magnetic fields beyond the timescale of several hours. Therefore, theoretical models are necessary to predict the behavior of magnetic fields on the timescales relevant to remanence acquired on planetesimals (hours to several million years Fu *et al.*, 2012; Carporzen *et al.*, 2011).

Magnetohydrodynamic models of protoplanetary disk magnetic fields are undergoing a period of intense development, with increasingly sophisticated numerical simulations that incorporate an ever more complete range of physical effects (Turner *et al.*, 2014). Such models predict that the dominant component of fields near the midplane in the inner solar system is toroidal, except during possible brief periods when the direction of this field component undergoes reversals (Bai and Stone, 2013). However, this and the radial components of the magnetic fields should not influence remanent magnetization acquired by meteorites over

timescales much longer than the orbital period. In contrast, a stable vertical magnetic field threading the disk may potentially be recorded as a stable magnetic field with paleointensity equal to the projection of the vertical field onto the planetesimal rotation axis. Because the strength and persistence of the vertical field is usually included as an input parameter in the MHD shearing box models used to simulate disk fields, such models cannot, by themselves, predict the intensity of these fields (e.g. Simon *et al.*, 2013a, 2013b). In the absence of such predictions, the total field intensities derived from Semarkona chondrules (5–50 μT) may be used as an approximate upper bound to the vertical magnetic field.

Because the vertical disk magnetic field may lead to recorded paleointensities in a range (0–50 μT) that overlaps significantly with dynamo field intensities inferred from both chondrites and achondrites (see Sections 9.2.1 and 9.2.2), the intensity of remanent magnetization itself cannot be used to distinguish between internal and external origins. On the other hand, because the solar nebula had a probable lifetime of less than ~5 Myr (Haisch *et al.*, 2001), while core dynamos, even in small bodies may persist for longer timescales (Sterenborg and Crowley, 2013), radiometric constraints on the age of magnetization potentially permit the exclusion of nebular magnetic fields as the cause of observed late-formed remanence.

9.7 Summary

Remanent magnetization found in HED meteorites as well as in more primitive carbonaceous chondrites indicates that a stable magnetic field was present in their parent bodies in early solar system history. The lack of magnetization in the Semarkona LL chondrite and the NWA 7325 ungrouped meteorite suggest that dynamo fields were not universal and that differentiation alone may not be sufficient to produce a dynamo. Remagnetization mechanisms *in situ* and on Earth increase uncertainty in interpreting paleomagnetism and thereby necessitate the use of additional proxies to provide context.

Considering the meteoritic evidence that at least some planetesimals were magnetized, then at least some asteroids are also expected to be magnetized. However, asteroidal magnetic fields have still not been unambiguously detected despite magnetometer flybys conducted near (21) Lutetia, (243) Ida, (951) Gaspra, (2867) Šteins, and (9969) Braille, and landings on the asteroid (433) Eros and the comet 67P/Cheryumov–Gerasimenkov. The most likely explanation is that the magnetization is nonunidirectional and thus weak at a distance.

Since environmental solar magnetic fields likely had a lifetime of less than ~5 Myr, paleomagnetism in meteorites suggests that core dynamo action provided the stable magnetic field source recorded as planetesimals cooled. Aluminum-26 was likely the primary heat source to cause the large-scale differentiation needed

to form a core. Above 950 °C, molten metal may have begun to percolate downward and form a core, although this process may have required even higher temperatures to partially melt the silicate. Core formation and size depended on the peak temperature and duration of heating, which in turn strongly depend on body size and accretion rate.

There is little literature dedicated specifically to planetesimal dynamos. However, modeling thus far has proven capable of explaining the field magnitude and duration inferred from paleomagnetic observation. The effect of core crystallization depends on the mode of solidification, which is largely unknown. Both inward and outward solidification in planetesimals is supported by meteoritic evidence. In the former scenario, a dynamo magnetic field could be preserved in iron meteorites; however, latent heat and light elements at the outer boundary of the core would inhibit convection, reducing dynamo strength and longevity. Outward solidification or solidification in an iron "snow" regime would enhance convection and strengthen the field.

Acknowledgments

The authors thank Gerald Schubert for his constructive comments on an early draft.

References

Acuña, M. H., Anderson, B. J., Russell, C.T., *et al.* 2002. NEAR magnetic field observations at 433 Eros: First measurements from the surface of an asteroid. *Icarus*, **155**, 220–228.

Acuña, M. H., Kletetschka, G., and Connerney, J. E. P. 2008. Mars' crustal magnetization: A window into the past. In *The Martian Surface: Composition, Mineralogy, and Physical Properties*, ed. J.F. Bell. Cambridge: Cambridge University Press, 242–262.

Anderson, B. J., Johnson, C. L., Korth, H., *et al.* 2011. The global magnetic field of Mercury from MESSENGER orbital observations. *Science*, **333**, 1859–1862.

Asphaug, E. 2010. Similar-sized collisions and the diversity of planets. *Chemie der Erde*, **70**, 199–219.

Auster, H. U., Richter, I., Glassmeier, K.-H., *et al.* 2010. Magnetic field investigations during Rosetta's 2867 Šteins flyby. *Planetary and Space Science*, **58**, 1124–1128.

Auster, H. U., Apathy, I., Berghofer, G., *et al.* 2015. The nonmagnetic nucleus of comet 67P/Churyumov–Gerasimenko. *Science*, **349**, aaa5102-1.

Bai, X.-N. and Stone, J. M. 2013. Wind-driven accretion in protoplanetary disks. I. Suppression of the magnetorotational instability and launching of the magnetocentrifugal wind. *Astrophysical Journal*, **769**, 76.

Baumgartel, K., Sauer, K., Story, T. R., and Mckenzie, J. F. 1997. Solar wind response to a magnetized asteroid: Linear theory. *Icarus*, **129**, 94-105.

Bland, P. A., Collins, G. S., Davison, T. M., *et al.* 2014. Pressure–temperature evolution of primordial solar system solids during impact-induced compaction. *Nature Communications*, **5**, 5451.

Blanco-Cano, X., Omidi, N. and Russell, C. T. 2003. Hybrid simulations of solar wind interaction with magnetized asteroids: Comparison with Galileo observations near Gaspra and Ida. *Journal of Geophysical Research*, **108**, 1216.

Brett, R. and Bell, P. M. 1969. Melting relations in the Fe-rich portion of the system Fe–FeS at 30 kb pressure, *Earth and Planetary Science Letters*, **6**, 479–482.

Bryson, J. F. J., Nichols, C. I. O., Herrero-Albillos, J., *et al.*, 2015. Long-lived magnetism from solidification-driven convection on the pallasite parent body. *Nature*, **517**, 472–475.

Burke, B. F. and Franklin, K. L. 1955. Observations of a variable radio source associated with the planet Jupiter. *Journal of Geophysical Research*, **60**, 213–217.

Butler, R. F. 1972. Natural remanent magnetization and thermomagnetic properties of Allende meteorite. *Earth and Planetary Science Letters*, **17**, 120–128.

Carporzen, L., Weiss, B. P., Elkins-Tanton, L. T. *et al.* 2011. Magnetic evidence for a partially differentiated carbonaceous chondrite parent body. *Proceedings of the National Academy of Sciences of the United States of America*, **108**, 6386–6389.

Cerantola, V., Walte, N. P., and Rubie, D. C. 2015. Deformation of a crystalline olivine aggregate containing two immiscible liquids: Implications for early core–mantle differentiation. *Earth and Planetary Science Letters*, **417**, 67–77.

Chabot, N. L. and Haack, H. 2006. Evolution of asteroidal cores. In *Meteorites and the Early Solar System II*, ed. D. S. Lauretta and H. Y. McSween, Jr. Tucson, AZ: University of Arizona Press, 747–771.

Chan, K. H., Zhang, K., Li, L., and Liao, X. 2007. A new generation of convection-driven spherical dynamos using EBE finite element method. *Physics of the Earth and Planetary Interiors*, **163**, 1–4.

Christensen, U. R., 2010. Dynamo scaling laws and applications to the planets. *Space Science Reviews*, **152**, 565–590.

Christensen, U. R. 2014. Iron snow dynamo models for Ganymede. *Icarus*, **247**, 248–259.

Christensen, U. R. and Wicht, J. 2007. Numerical dynamo simulations. In *Treatise on Geophysics*, ed. P. L. Olson. Amsterdam: Elsevier, 245–282.

Christensen, U. R., Olson, P., and Glatzmaier, G. 1999. Numerical modeling of the geodynamo: A systematic parameter study. *Geophysical Journal* International, **138**, 393–409.

Christensen, U. R., Holzwarth, V., and Reiners, A. 2009. Energy flux determines magnetic field strength of planets and stars. *Nature*, **457**, 167–169.

Cisowski, S. M. 1991. Remanent magnetic properties of unbrecciated eucrites. *Earth and Planetary Science Letters*, **107**, 173–181.

Collinson, D. W. and Morden, S. J. 1994. Magnetic-properties of howardite, eucrite and diogenite (HED) meteorites: Ancient mgnetizing fields and meteorite evolution. *Earth and Planetary Science Letters*, **126**, 421–434.

Cournède, C., Gattacceca, J., Zanda, B., and Rochette, P. 2012. Magnetic study of CM chondrites. EGU General Assembly, Vienna, April 22–27, paper no. 9740.

Cournède, C., Gattacceca, J., and Rochette, P. 2014. Partial asteroid differentiation revealed by paleomagnetism of R-chondrite meteorites. EGU General Assembly. Vienna, April 27–May 2, paper no. 4155.

Cournède, C., Gattacceca, J., Gounelle, M., *et al.* 2015. An early solar system magnetic field recorded in CM chondrites. *Earth and Planetary Science Letters*, **410**, 62–74.

Cowling, T. G. 1934. The magnetic field of sunspots. *Monthly Notices of the Royal Astronomical Society*, **34**, 39–48.

Elkins-Tanton, L. T., Weiss, B. P., and Zuber, M. T. 2011. Chondrites as samples of differentiated planetesimals. *Earth and Planetary Science Letters*, **305**, 1–10.

Emmerton, S., Muxworthy, A. R., Hezel, D. C., and Bland, P. A. 2011. Magnetic characteristics of CV chondrules with paleointensity implications. *Journal of Geophysical Research*, **116**, E12007.

Fei, Y., Bertka, C. M., and Finger, L. W. 1997. High-pressure iron-sulfur compound, Fe_3S_2, and melting relations in the Fe–FeS system. *Science*, **275**, 1621–1623.

Fischer, S. R., Fu, R. R., Weiss, B. P., *et al.* 2013. Paleomagnetic detection of magnetic fields on a differentiated asteroid during the dynamo epoch. AGU Fall Meeting, San Francisco, December 9–13, abstract GP41D–1166.

Fu, R. R. and Elkins-Tanton, L. T. 2014. The fate of magmas in planetesimals and the retention of primitive chondritic crusts. *Earth and Planetary Science Letters*, **390**, 128–137.

Fu, R. R. and Weiss, B. P. 2012. Detrital remanent magnetization in the solar nebula. *Journal of Geophysical Research*, **117**, E02003.

Fu, R. R., Weiss, B. P., Shuster, D. L., *et al.* 2012. An ancient core dynamo in asteroid Vesta. *Science*, **338**, 238–241.

Fu, R. R., Lima, E. A., and Weiss, B. P. 2014a. No nebular magnetization in the Allende CV carbonaceous chondrite. *Earth and Planetary Science Letters*, **404**, 54–66.

Fu, R. R., Weiss, B. P., Lima, E. A., *et al.* 2014b. Solar nebula magnetic fields recorded in the Semarkona meteorite. *Science*, **346**, 1089–1092.

Gattacceca, J., Rochette, P., and Bourot-Denise, M. 2003. Magnetic properties of a freshly fallen LL ordinary chondrite: the Bensour meteorite. *Physics of the Earth and Planetary Interiors*, **140**, 343–358.

Gattacceca, J. and Rochette, P. 2004. Toward a robust normalized magnetic paleointensity method applied to meteorites. *Earth and Planetary Science Letters*, **227**, 377–393.

Gattacceca, J. Berthe, L. Boustie, M., *et al.* 2008. On the efficiency of shock magnetization processes. *Physics of the Earth and Planetary Interiors*, **166**, 1–10.

Greenstadt, E. W. 1971a. Conditions for magnetic interaction of asteroids with the solar wind. *Icarus*, **14**, 374–381.

Greenstadt, E. W. 1971b. Possible magnetic interaction of asteroids with the solar wind. *Proceedings of IAU Colloquium*, **12**, 567–575.

Grove, T. L. 1982. Use of exsolution lamellae in lunar clinopyroxenes as cooling rate speedometers: An experimental calibration. *American Mineralologist*, **67**, 251–268.

Goldstein, J. I., Scott, E. R. D. and Chabot, N. L 2009. Iron meteorites: Crystallization, thermal history, parent bodies, and origin. *Chemie der Erde*, **69**, 293–325.

Haack, H. and Scott, E. R. D. 1992. Asteroid core crystallization by inward dendritic growth. *Journal of Geophysical Research*, **97**, 14727–14734.

Haisch, K. E., Lada, E. A., and Lada, C. J. 2001. Disk frequencies and lifetimes in young clusters. *Astrophysical Journal Letters*, **553**, L153–L156.

Hauck, S. A., Aurnou, J. M., and Dombard, A. J. 2006. Sulfur's impact on core evolution and magnetic field generation on Ganymede. *Journal of Geophysical Research*, **111**, E09008.

Kerswell, R. R. 1993. The instability of precessing flow. *Geophysical & Astrophysical Fluid* Dynamics, **72**, 107–144.

Kivelson, M. G., Bargatze, L. F., Khurana, K. K., *et al.* 1993. Magnetic field signatures near Galileo's closest approach to Gaspra. *Science*, **261**, 331–334.

Kivelson, M. G., Wang, Z., Joy, S. P., *et al.* 1995. Solar wind interaction with small bodies. 2. What can Galileo's detection of magnetic rotations tell us about Gaspra and Ida. *Advances in Space* Research, **16**, 47–57.

Kivelson, M. G., Khurana, K. K., Russell, C. T., *et al.* 1996. Discovery of Ganymede's magnetic field by the Galileo spacecraft. *Nature*, **384**, 537–541.

Kruijer, T. S., Touboul, M., Fischer-Gödde, M., *et al.* 2014. Protracted core formation and rapid accretion of protoplanets. *Science*, **344**, 1150–1154.

Kullerud, G. and Yoder, H. S. 1959. Pyrite stability relations in the Fe–S system. *Economic Geology*, **54**, 533–572.

Laneuville, M., Wieczorek, M. A., Breuer, D., *et al.* 2014. A long-lived lunar dynamo powered by core crystallization. *Earth and Planetary Science Letters*, **401**, 251–260.

Le Bars, M., Wieczorek, M. A., Karatekin, O., Cebron, D., and Laneuville, M. 2011. An impact-driven dynamo for the early Moon. *Nature*, **479**, 215–218.

McCoy, T. J., Keil, K., Muenow, D.W., and Wilson, L. 1997. Partial melting and melt migration in the acapulcoite–lodranite parent body. *Geochimica et Cosmochimica Acta*, **61**, 639–650.

Monteux, J., Jellinek, A. M., and Johnson, C. L. 2011. Why might planets and moons have early dynamos? *Earth and Planetary Science Letters*, **310**, 349–359.

Morden, S. J. 1992. A magnetic study of the Millbillillie (eucrite) achondrite: Evidence for dynamo-type magnetising field. *Meteoritics*, **27**, 560–567.

Morden, S. J. and Collinson, D. W. 1992. The implications of the magnetism of ordinary chondrite meteorites. *Earth and Planetary Science Letters*, **109**, 185–204.

Nagata, T. 1979. Natural remanent magnetization of the fusion crust of meteorites. *Memoirs of National Institute of Polar Research*, **15**, 253–272.

Narayan, C. and Goldstein, J. I. 1982. A dendritic solidification model to explain Ge–Ni variations in iron meteorite chemical groups. *Geochimica et Cosmochimica Acta*, **46**, 259–268.

Ness, N. F. 2010. Space exploration of planetary magnetism. *Space Science Reviews*, **152**, 5–22.

Nimmo, F. 2009. Energetics of asteroid dynamos and the role of compositional convection. *Geophysical Research Letters*, **36**, L10201.

Omidi, N., Blanco-Cano, X., Russell, C. T., Karimabadi, H., and Acuna, M. 2002. Hybrid simulations of solar wind interaction with magnetized asteroids: General characteristics. *Journal of Geophysical Research*, **107**, 1487.

Pesonen, L. J., Terho, M., and Kukkonen, I. T. 1993. Physical properties of 368 meteorites: Implications for meteorite magnetism and planetary geophysics. *Proceedings of the NIPR Symposium on Antarctic Meteorites*, **6**, 401–416.

Richter, I., Brinza, D. E., Cassel, M., *et al.* 2001. First direct magnetic field measurements of an asteroidal magnetic field: DS1 at Braille. *Geophysical Research Letters*, **28**, 1913–1916.

Richter, I., Auster, H. U., Glassmeier, K. H., *et al.* 2012. Magnetic field measurements during the Rosetta flyby at asteroid (21) Lutetia. *Planetary and Space Science*, **66**, 155–164.

Rückriemen, T., Breuer, D., and Spohn, T. 2015. The Fe snow regime in Ganymede's core: A deep-seated dynamo below a stable snow zone. *Journal of Geophysical Research: Planets*, **120**, 1095–1118.

Scheinberg, A., Fu, R. R., Elkins-Tanton, E. T., and Weiss, B. P. 2015. Asteroid differentiation: melting and large-scale structure. In *Asteroids IV*, ed. P. Michel, F. DeMeo, and W. F. Bottke. Tucson, AZ: University of Arizona Press, 533–552.

Scheinberg, A., Elkins-Tanton, E. T., Schubert, G., and Bercovici, D. 2016. Core solidification and dynamo evolution in a mantle-stripped planetesimal. *Journal of Geophysical Research: Planets*, **121**, 2–20.

Scherstén, A., Elliott, T., Hawkesworth, C., Russell, S., and Masarik, J. 2006. Hf,W evidence for rapid differentiation of iron meteorite parent bodies. *Earth and Planetary Science Letters*, **241**, 530–542.

Sears, D. W. 1975. Temperature gradients in meteorites produced by heating during atmospheric passage. *Modern Geology*, **5**, 155–164.

Shea, E. K., Weiss, B. P., Cassata, W. S., *et al.* 2012. A long-lived lunar core dynamo. *Science*, **335**, 453–456.

Simon, J. B., Bai, X.-N., Stone, J. M., Armitage, P. J., and Beckwith, K. 2013a. Turbulence in the outer regions of protoplanetary disks. I. Weak accretion with no vertical magnetic flux. *Astrophysical Journal*, **764**, 66.

Simon, J. B., Bai, X.-N., Stone, J. M., Armitage, P. J., and Beckwith, K. 2013b. Turbulence in the outer regions of protoplanetary disks. II. Strong accretion driven by a vertical magnetic field. *Astrophysical Journal*, **775**, 73.

Sterenborg, M. G. and Crowley, J. W. 2013. Thermal evolution of early solar system planetesimals and the possibility of sustained dynamos. *Physics of the Earth and Planetary Interiors*, **214**, 53–73.

Stevenson, D. J. 2001. Mars' core and magnetism. *Nature*, **412**, 214–219.

Stevenson, D. J. 2003. Planetary magnetic fields. *Earth and Planetary Science Letters*, **208**, 1–11.

Stöffler, D., Keil, K., and Scott, E. R. D. 1991. Shock metamorphism of ordinary chondrites. *Geochimica et Cosmochimica Acta*, **55**, 3845–3867.

Suavet, C., Gattacceca, J., Rochette, P., *et al.* 2009. Magnetic properties of micrometeorites. *Journal of Geophysical Research*, **114**, B04102.

Sugiura, N., Lanoix, M., and Strangway, D. W. 1979. Magnetic fields of the solar nebula as recorded in chondrules from the Allende meteorite. *Physics of the Earth and Planetary Interiors*, **20**, 342–349.

Swindle, T. D. 1998. Implications of iodine-xenon studies for the timing and location of secondary alteration. *Meteoritics & Planetary Science*, **33**, 1147–1155.

Tarduno, J. A., Cottrell, R. D., Nimmo, F., *et al.* 2012. Evidence for a dynamo in the main group pallasite parent body. *Science*, **338**, 939–942.

Tarduno, J. A. and Cottrell, R. D. 2012. Single crystal paleointensity analyses of olivine–diogenites: Implications for a past Vestan dynamo. *Lunar and Planetary Science Conference*, **43**, 2663.

Tilgner, A. 2005. Precession driven dynamos. *Physics of Fluids*, **17**, 034104.

Tomkins, A. G., Mare, E. R., and Raveggi, M. 2013. Fe-carbide and Fe-sulfide liquid immiscibility in IAB meteorite, Campo del Cielo: Implications for iron meteorite chemistry and planetesimal core compositions. *Geochimica et Cosmochimica Acta*, **117**, 80–98.

Turner, N. J. Fromang, S., Gammie, C., *et al.*, 2014. Transport and accretion in planet-forming disks. In *Protostars and Planets VI*, ed. H. Beuther, R. S Klessen, C. P Dullemond, and T. Henning. Tucscon, AZ: University of Arizona Press, 411–434.

Uehara, M., Gattacceca, J., Leroux, H., Jacob, D., and van der Beek, C. J., 2011. Magnetic microstructures of metal grains in equilibrated ordinary chondrites and implications of paleomagnetism of meteorites. *Earth and Planetary Science Letters*, **306**, 241–252.

Wasilewski, P. 1981. New magnetic results from Allende C3(V). *Physics of the Earth and Planetary Interiors*, **26**, 134–148.

Wasilewski, P., Acuña, M. H., and Kletetschka G. 2002. 433 Eros: Problems with the meteorite magnetism record in attempting an asteroid match. *Meteoritics & Planetary Science*, **37**, 937–950.

Wei, X., Arlt, R., and Tilgner, A. 2014. A simplified model of collision-driven dynamo action in small bodies. *Physics of the Earth and Planetary Interiors*, **231**, 30–38.

Weisberg, M. K., McCoy, T. J., and Krot, A. N., 2006. Systematics and evaluation of meteorite classification. In *Meteorites and the Early Solar System II*, ed. D. S. Lauretta and H. Y. McSween, Jr. Tucson, AZ: University of Arizona Press, 19–52.

Weiss, B. P. and Tikoo, S. M. 2014. The lunar dynamo. *Science*, **346**, 1246753, doi: 10.1126/science.1246753.

Weiss, B. P., Berdahl, J. S., Elkins-Tanton, L. T., *et al.*, 2008. Magnetism on the angrite parent body and the early differentiation of planetesimals. *Science*, **322**, 713–716.

Weiss, B. P., Gattacceca, J., Stanley, S., Rochette, P., and Christensen, U. R. 2010. Paleomagnetic records of meteorites and early planetesimal differentiation. *Space Science Reviews*, **152**, 341–390.

Weiss, B. P., Wang, H., Downey, B. G., *et al.*, 2014. An unmagnetized early planetary body. AGU Fall Meeting, San Francisco, December 15–19, abstract GP51B–3733.

Williams, Q. 2009. Bottom-up versus top-down solidification of the cores of small solar system bodies: Constraints on paradoxical cores. *Earth and Planetary Science Letters*, **284**, 564–569.

Yang, J., Goldstein, J. I., and Scott, E. R. D. 2008. Metallographic cooling rates and origin of IVA iron meteorites. *Geochimica et Cosmochimica Acta*, **72**, 3043–3061.

Yang, J., Goldstein, J. I., Michael, J. R., Kotula, P. G., and Scott, E. R. D. 2010. Thermal history and origin of the IVB iron meteorites and their parent body. *Geochimica et Cosmochimica Acta*, **74**, 4493–4506.

Yoshino T., Walter M. ., and Katsura T. 2003. Core formation in planetesimals triggered by permeable flow. *Nature*, **422**, 154–157.

Zhan, X., Zhang, K., and Zhu, R. 2011. A full-sphere convection-driven dynamo: Implications for the ancient geomagnetic field. *Physics of the Earth and Planetary Interiors*, **187**, 328–335.

Ziegler, L. B. and Stegman, D. R. 2013. Implications of a long-lived basal magma ocean in generating Earth's ancient magnetic field. *Geochemistry, Geophysics,* Geosystems, **14**, 4735–4742.

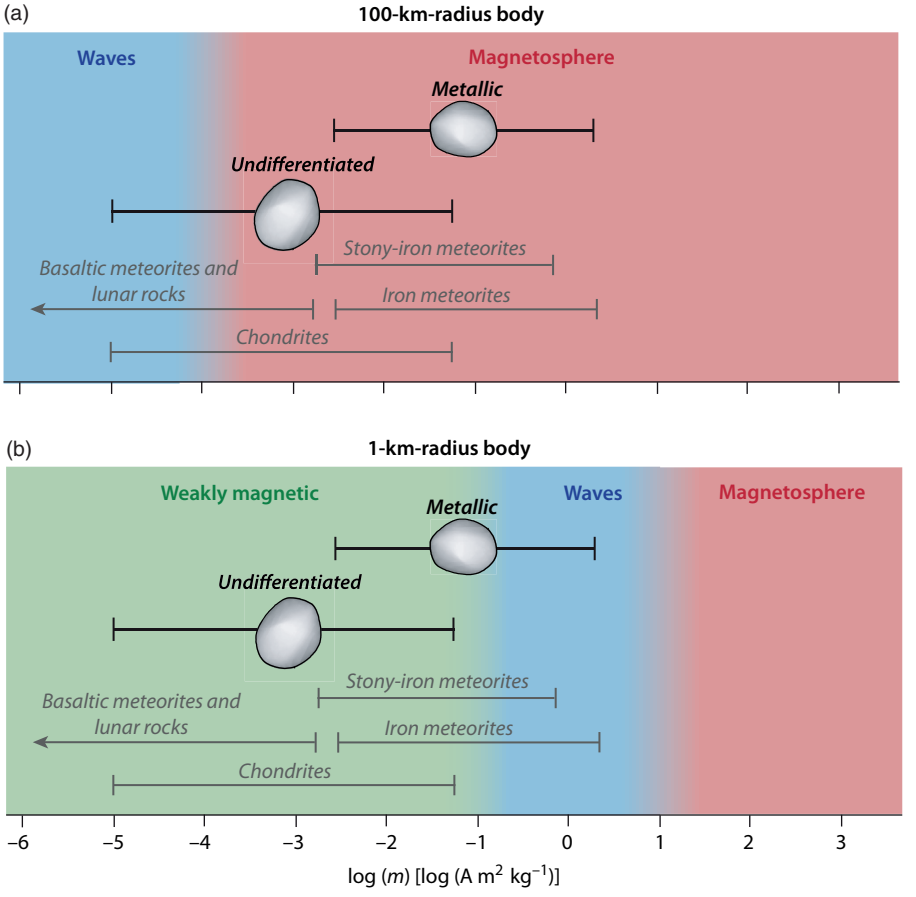

For caption, see figure 9.2 in the main text.

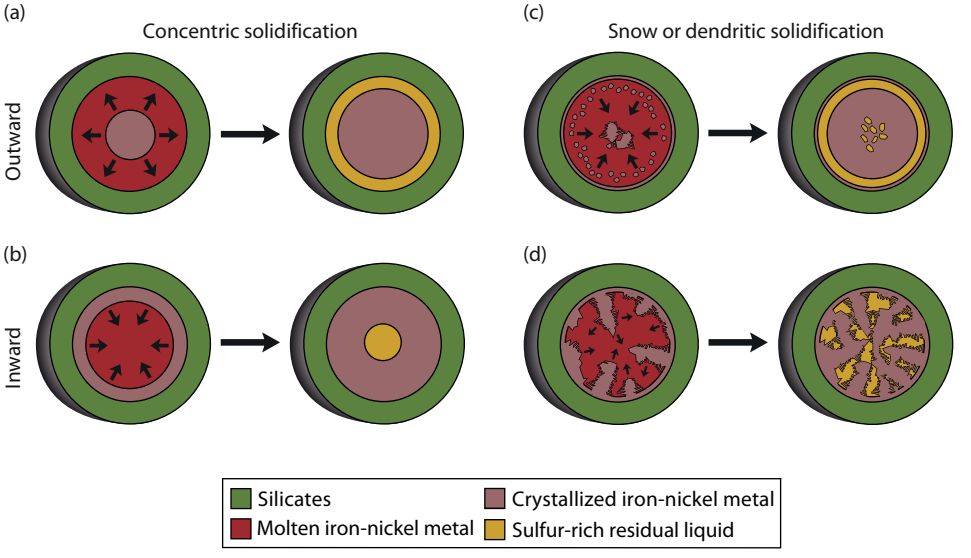

For caption, see figure 9.3 in the main text.